(18)

EXAMINATION OF IRRADIATED CONTROL RODS AT MAGNOX ELECTRIC

Presentation to the European Working Group
Hot Laboratories & Remote Handling

Plenary Meeting - June 5-6

Studsvik, Sweden

Prepared by Magnox Electric Staff

Presented by Mr M D Thornley
Nuclear Systems Manager
Technology & Central Engineering Division

MAGNOX

CONTENTS

1. INTRODUCTION

In order to support the continued safe and economic operation of Magnox Electric's twelve CO_2 cooled Magnox reactors it is essential that correct functioning of control rod systems is maintained. Ageing mechanisms associated with the radiological and high temperature environment can lead to rod distortion and structural cracking and these effects are heavily influenced by the construction and manufacturing details of the rods.

Techniques developed at the Magnox Electric Nuclear Laboratories at Berkeley have provided detailed analysis of the processes associated with control rod ageing and have enabled operational safety cases to be maintained for all reactors.

This paper describes the hot cell facilities at Berkeley and reviews techniques applied to the mechanical, metallographic and microstructural aspects of control rod examination.

2. BERKELEY HOT CELL FACILITIES, AN OVERVIEW DESCRIPTION

First established in 1962 by the CEGB* as Berkeley Nuclear Laboratories, and now named 'Berkeley Centre', the Hot Cell Facility has since been extended and refurbished and now provides a full PIE capability for fuel and irradiated components. Mechanical, chemical, radiological and microstructural analyses are carried out in the facility.

The shielded caves and cells have, in the recent past, been refurbished to modern standards and much of the equipment and specialised examination/analytical techniques lend themselves to a wide range of materials originating from modern reactor systems.

Magnox Electric, and its predecessor companies, Nuclear Electric plc and the CEGB, have concentrated use of the facilities on fuel and materials from its own gas cooled reactors, however, where opportunities arise Magnox Electric is now applying these techniques to a range of water reactor materials.

The facility includes six large concrete caves, each served by twin Walischmiller manipulators and 25 cells of a variety of sizes and constructions. Access for irradiated materials to the Facility is either by direct posting, or via a pond. A pneumatically operated 'rabbit' system provides automatic transfer of small components between the caves and cells.

* Central Electricity Generating Board

At Berkeley Centre fully shielded, computer controlled mechanical test facilities have been established with conditions to suit core component surveillance programmes from any reactor system. Additionally, a fully-shielded computer controlled milling machine provides a capability for supplying a range of test pieces from virtually any reasonably sized component.

A microstructural investigations unit has been established adjacent to the main active area with a wide range of techniques such as FEGSTEM, Field Emission Auger Spectroscopy, XPS/SIMS and high voltage (S)TEM available for the rapid examination of active fuel and components. An innovative and flexible sample preparation capability provides strong support for this unit. A fully Shielded Scanning Electron Microscope has also been installed which is capable of examination and analysis of highly active sections which can be accepted directly from the other cave or cell facilities.

The in-cave fuel examination facilities, metallographic suite and electron optical examination suite all have the capability for digital storage and electronic retrieval of images to provide a faster response to search demands, quantitative image analysis and image processing to improve the quality of hard copy presentations.

3. CONTROL ROD ISSUES

Magnox Power Stations use natural Uranium fuel with magnesium alloy cladding, CO_2 coolant and graphite moderator. Typical inlet and outlet temperatures are 190°C and 360°C, respectively. Primary and secondary control rods have cylindrical boron steel inserts, retained by a ferritic or austenitic steel sheath, Figures 1,2. The insert has a typical boron content of 3-4wt% and is around 5mm thick. The sheath has an outer diameter of 8cm and wall thickness of 2-3mm. Design is station-specific. Slow neutron absorption by the boron steel insert leads to significant swelling as ^{10}B transmutes to Li and He. The sheath must retain sufficient ductility to accommodate this swelling. In 1992 a control rod removed from the Wylfa station, in Wales, was found to have suffered sheath damage. A substantial programme of Post Irradiation Examination (PIE) was established immediately for this control rod in order to establish the reasons for the apparent loss of sheath ductility.

Subsequently, detailed examination of a number of control rods has been undertaken, including both mild and stainless steel sheathed designs. The examination and test programmes have investigated the mechanical and microstructural features of the irradiated components as well as irradiation history.

One of the requirements was to make a Transmission Electron Microscope (TEM) examination of the sheath microstructure. Comparative microstructural observations were also conducted on other intact, control rods that exhibited significant sheath deformation, due to insert swelling, but had retained full mechanical integrity.

An additional area for study on stainless steel materials was the potential for sensitisation in the event of chromium depletion at grain boundaries as a result of irradiation induced migration. Examinations using the FEGSTEM (Field Emission Gun Scanning Transmission Electron Microscope) are able to interrogate the compositional variation across grain boundaries in great detail to determine the local chemical composition and indicate the vulnerability of the material to intergranular cracking.

Using information gained from these examinations, in particular the presence of copper precipitates in sheath material of the Wylfa control rod, has enabled specific conclusions regarding the operating temperatures to be made which have supported the safety case for the reactivity control systems.

4. PREPARATION AND MECHANICAL TESTING

Control rod sections were delivered to Berkeley as cut lengths of approximately 1m.

On receipt, the rods were visually examined, including examination of the bore by a remote camera probe to identify the extent of surface cracking and any other surface characteristics.

Dimensional checks on components were carried out to determine the extent and orientation of swelling or other distortion. The sheath wall thickness was measured on each specimen at ten equispaced positions using a micron resolution transducer mounted on a microscope stage. Measurements were at a magnification of x500. Care was taken to ensure that measurements were taken perpendicular to the sheath surface in each case and results, together with their mean and standard deviation were calculated. These detailed analyses allowed the effects of swelling to be differentiated from manufacturing variations in the welded structure.

Morphology of the surface oxide layer was observed revealing, in general a thin reflective grey layer. This impression was confirmed by optical metallography which identified typical layers measured from 3μm to 25μm.

Following the macroscopic examinations a cutting programme was designed and the component divided into specimen samples (Fig. 3) using the in-cell hacksaw and slitting machine tools. Those samples identified for tensile testing were finish machined on the in cell CNC milling machine.

Tensile testing was performed on a Schenk servo mechanical frame which provides, in cell, controlled strain rate. A slow strain rate of $\sim 6x10^{-4}s^{-1}$ was chosen to enable any rapid discontinuities in materials performance which may indicate brittle behaviour to be fully recorded. The ductility/notch sensitivity was further characterised by carrying out tests on both plain and notched tensile specimens.

Variations in sheath hardness were measured at various axial positions and in the weld region using an Equotip dynamic hardness tester or Vickers machine with a 5kg or 10kg load. Whilst scatter in results using the Equotip device was relatively low, again the importance of ensuring that the probe was held normal to the specimen surface was apparent.

Fractography was carried out on relevant components using the Joel 6100 fully Shielded Scanning Electron Microscope. This equipment, which incorporates x-ray microanalysis capability enabled the whole of the circumference of the irradiated component to be examined. Surface features such as oxidation, indicating crack age, and fracture characteristics such as chevron marks and/or brittle/ductile behaviours can be identified. Examination of the full scale component in the shielded SEM provided data to enable specific features of interest to be identified for further detailed microstructural analysis, as described below.

Specimens for optical metallography were cut from the sheath to more closely examine crack tips and grain structure. Specimens were mounted, ground and mechanically polished to 1μm before attack polishing and etching with 1 % nital to enhance microstructural contrast.

Optical examinations were carried out using the in-cell microscope which incorporates CCD TV camera viewing, allowing image storage/retrieval and analysis.

5. MICROSTRUCTURAL EXAMINATION

Further understanding of the materials performance and its operational history was gained through the use of the range of electron optical tools which are integrated into the Berkeley active facility. It was particularly important to seek indications from the material regarding the temperature at which any structural effects had occurred, and to determine the neutron dose exposure. This was achieved by employing a combination of techniques, in particular TEM and Auger spectroscopy and SIMS.

5.1 Compositional Analysis

Prior to detailed analysis of microstructural composition, the bulk composition of rod materials was determined to enable comparison against design specifications to be made. This analysis was carried out in the Jeol JXA 8600 electron microprobe using wavelength dispersive analysis. The 3mm diameter specimens were ground and electropolished prior to the analysis. The count rates from individual elements were converted into mass fractions, the instruments operation being checked by examination of an adjacent steel standard of known composition.

5.2 Transmission Electron Microscopy

Examination of features such as dislocation loops, precipitates, voids and elemental migration requires the use of the transmission electron microscope.

Preparation of high quality specimens is critical to the success of this examination and this can be particularly challenging for highly active components such as those containing significant Cobalt concentrations.

3mm diameter discs were punched in cell from sheath slices which had been cut to approximately 1mm thickness. For the high Cobalt stainless steel materials and those recently discharged (typically ~ 1 month after removal from the reactor) dose rates from the discs were in excess of 10mSv/hr and these could not be handled via the usual glove box route.

Specimens were mechanically ground in cell to reduce their thickness to approximately 100μm before posting to the active electron optics suite for perforation to electron transparency by electropolishing in a solution of 5% perchloric acid in methanol at around -60°C.

These specimens are suitable for examination in the Jeol 3010 TEM, however for the high activity samples, the beam-off signal detected by the energy dispersive x-ray microanalysis (EDX) detectors precluded x-ray microanalysis.

Reduction in sample activity was achieved by producing a composite specimen comprising a 1mm diameter disc inserted into a 3mm outer diameter unirradiated annulus. Following perforation of the 1mm disc successful x-ray microanalysis was performed.

Microchemical Analysis was performed using a Vacuum Generators HB501 Field Emission Gun Scanning Transmission Electron Microscope (FEGSTEM). This operates at 100KeV and allows microanalysis to be performed with a spatial resolution below 1.5-2nm.

The TEM/FEGSTEM examination was of particular significance in determining the causes for reduced sheath ductility which resulted in cracking of the sheath under the influence strain induced by insert swelling.

5.3 Neutron Dose Determination

Measurement of Boron 10:Boron 11 ratio on polished 'matchstick' samples by Secondary Ion Mass Spectrometry (SIMS) on the Kratos XSAM 330 enables the neutron dose to be calculated from the reduction in ^{10}B through the reaction

$$^{10}B + n \rightarrow {}^{7}Li + {}^{4}He$$

Particular care to avoid edge effects and the use of oxygen sputtering to eliminate effects associated with ^{40}Ar activation provided a dose profile which aligned closely with calculated values from MonteCarlo methods of typically 10×10^{20} n/cm^2 - 2×10^{21} n/cm^2.

6. CASE STUDY OF WYLFA CONTROL ROD EXAMINATIONS

As described in Section 3, the issues arising from operationally observed defects on the control rod from Wylfa were of particular significance. The materials investigation into this component is reviewed below.

6.1 Hardness Testing

Hardness testing of the failure origin of the control rod gave values of 241-246 HV at 5Kg and 243-249 at 10Kg load. By comparison, hardness measurements on the surfaces of unused control rods from the same batch gave value of 120-130 HV, indicating a significant hardening in service.

6.2 EPMA Measurements

EPMA measurements from the lightly electropolished discs from the two control rods sheaths examined are reproduced below.

EPMA Composition Measurements of Control Rod Sheath Material

	Copper	Silicon	Aluminium	Manganese
Failed Sheath	0.32-0.38	0.13-0.16	Not detected	0.51-0.52
Intact Sheath	0.11-0.15	0.28	0.03*	0.11-0.1

* = Calculated using counts relative to those on a standard low alloy steel sample with 0.008wt% Aluminium

6.3 Examination of Boron Steel Insert Material

Figure 4 shows an image of a thin foil prepared from the boron steel insert material from the damaged control rod. The image is slightly over focused. This produces dark Fresnel fringe contrast around matrix He bubbles, which have a mean diameter of approximately 2nm. The electron beam direction is close to <001>. At this orientation, alignment of the bubbles along <100> is apparent. Swelling of the insert at this position in the component is estimated to be around 4%.

6.4 TEM Observations of Sheath Material from Damaged Control Rod (Figure 5)

The Joel 3010 TEM has an operating voltage of 300 KeV and provides high quality imaging of microstructural features in magnetic materials. The general microstructure of the failed material was comparatively uniform and clean. A few small areas of pearlite were observed. Stringers of manganese silicate were present, the largest of which crossed several grain boundaries. The "non-loop" dislocation density within grains was low. Figure 5 (top) shows a typical area. There is a size-distribution of dislocation loops, from several tens of nanometres down to a few nanometres. At the bottom of the size range the dislocation loops are virtually indistinguishable from copper precipitates. The electron beam is close to a <100> direction in the grain being examined so that contrast is due to diffraction from two (100) sets of planes that are aligned nearly edge-on. Diffraction contrast is somewhat away from the Bragg condition for the two sets of planes, so fine-scale microstructural features can be seen with good resolution in the image. Dislocation loops in irradiated ferritic steel are known to lie predominantly on {100} planes, so that for orientation of Figure 2, 2/3 of loops are expected to be viewed edge-on and 1/3 to lie in the plane of the foil.

In order to confirm the identification of copper precipitates the sample was examined in the FEGSTEM. Over forty precipitates were examined by EDS. The great majority of these were identified as copper, by the presence of copper and iron in the spectra obtained. There is always a strong iron signal as the electron beam must pass through matrix above and below each precipitate. The copper precipitates are typically a few nanometres in diameter while the sample thickness in the region being examined would typically be several tens of nanometres. Some copper sulphides were also present, as expected in this type of material, along with one or two aluminium-rich particles.

Measurements were made of 20 loops and precipitates in an area from the field of Figure 5, directly from the negative of a dark-field image, using a standard 10x Lupe. In the case of non-circular dislocation loops and precipitates, the longest dimension was measured. Average diameters derived for loops and precipitates were ~4nm and ~12nm, respectively.

The control rod was known to have had an operating life of 25 years (t_{CR} ~ 130,000 hours). The mean copper precipitate diameter measured for the damaged rod material gives an operating temperature estimate of 285° ±15°C, using the expression

$$\frac{1}{T_{CR}} = \frac{1}{623} + \frac{k}{E} \cdot Ln \frac{t_{cr}}{t_{623}} \qquad \text{(Ref.1)}$$

where T_{CR} = Control rod operating temperature, °K
K = Boltzman constant, 8.6 x 10^{-5}eV/K
E = Activation energy for copper in iron alloys, 2.2eV
t_{623} = Time to produce precipitates at 623°K

The uncertainty range arises from lack of knowledge of the size distribution of any precipitates present at start-of-life and variation in published values of activation energies for the process.

Sheath material was also examined from near the top of the control rod, at a position constrained to an operating temperature close to the outlet gas temperature. At this temperature, the copper content is well above the solubility limit, and precipitate nucleation and growth is diffusion controlled. Examination of this material showed a clean microstructure and low dislocation density and a uniform dispersion of copper precipitates, with a mean diameter of ~18nm. This suggests an operating temperature of 335±15°. This position on the control rod was exposed to a low neutron flux. No dislocation loops were expected to be present and none were observed.

6.5 Examination of Intact Sheath Material

As described above, TEM foils were also prepared from sheath material from the position on a second control rod where significant insert swelling had been accommodated without loss of integrity of the sheath material. The purpose of this was to make a direct comparison with the microstructure of the high swelling bottom end of the damaged rod. From the EPMA results, it was known that this sheath material had approximately half the copper content, double the silicon and less than a quarter of the manganese content of the failed sheath. In addition, the intact sheath had a very significant aluminium content. For the failed material, the aluminium content was below the detection limit.

TEM examination revealed a microstructure that was consistent with known composition and assumed operating conditions. Non-loop dislocation density was variable within the material but generally higher than had been observed in the failed material. Both dislocation loop and precipitate densities were considerably lower. In areas with a significant density of line dislocations, loops were smaller and there was definite evidence of interaction between the two dislocation types, Figure 5 (bottom).

The confirmation of an operating temperature at the failure region of the control rod of ~285°C as a primary contributory factor in the loss of sheath ductility enabled a clear safety case to be established for the operation of all other rods at the normal temperature of ~330°C.

7. OBSERVATIONS FROM STAINLESS STEEL SHEATHED RODS

In addition to investigations of strain and swelling related effects in ferritic rods, stainless steel materials were examined to determine the effect of chromium depletion at gain boundaries using the FEGSTEM.

Figures 6 and 7 illustrate a composition profiles taken from different control rods. Whilst the results from Station 1 clearly indicate significant chromium depletion, this effect in the sample shown in Figure 7 is much less severe. Investigations at Berkeley Centre have indicated a strong relationship between chromium migration and the presence of molybdenum which appears to serve as an inhibitor to this process.

TEM observations also enable the voidage volume fraction to be calculated, which may typically be around 0.03% (Figure 8). This value is fully acceptable for Magnox reactors where available clearances for control rod movement are generally much larger than those in water reactors. Composition of 'void' inclusions can be interrogated using the EELS (Electron Energy Loss Spectroscopy) facility on the FEGSTEM.

8. CONCLUSIONS

Understanding of the complex interaction of materials properties, operating environment and irradiation history of control rods demands the application of a wide range of tools and techniques to ensure that processes are understood and future performance adequately predicted.

8. ACKNOWLEDGEMENTS

The assistance of Dr J Walmsley, Dr P Spellward, Dr T Gilmour, Dr J Tyler and other Magnox Electric staff in the production of this paper is gratefully acknowledged.

REFERENCES

1. Walmsley J C, Fisher S B and Spellward P. 'Microstructural and Microchemical Characterisation of Ferritic Ex-Service Magnox Control Rod Material.' Effects of Radiation on Materials: 18th International Symposium, ASTM STP 1325, Randy K Nanstad, Ed, American Society for Testing and Materials, 1996.

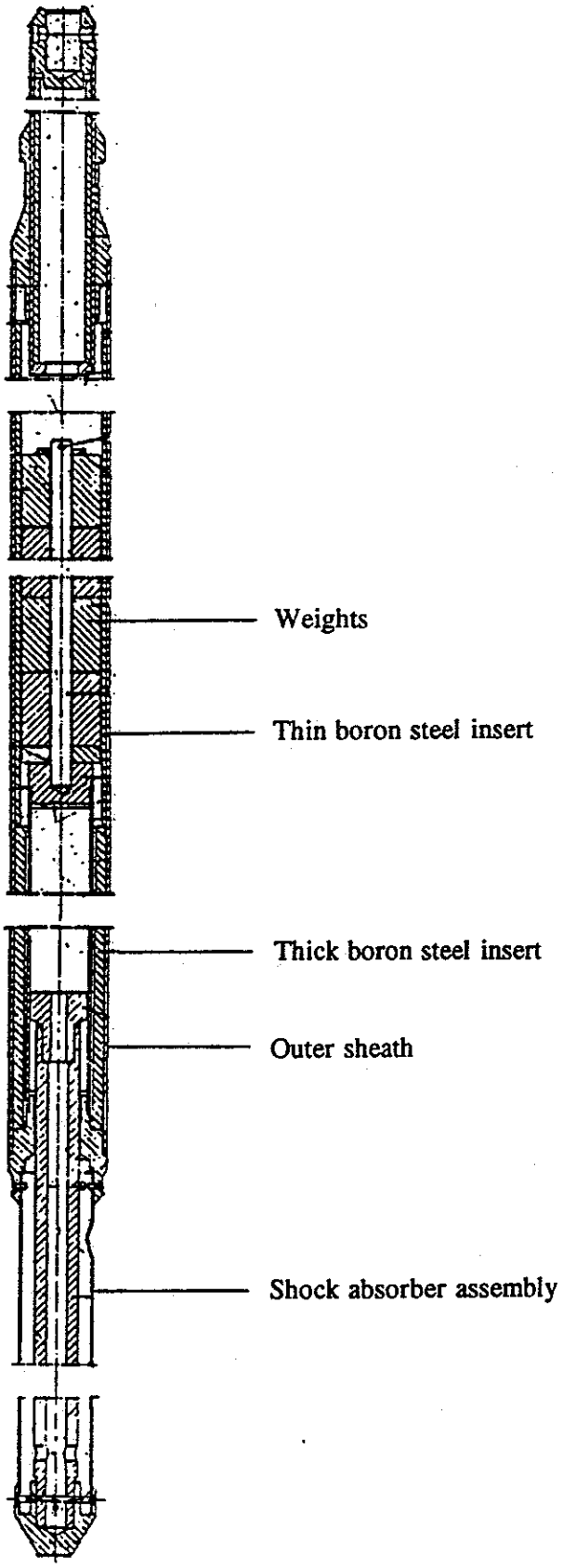

Figure 1: Diagram of control rod

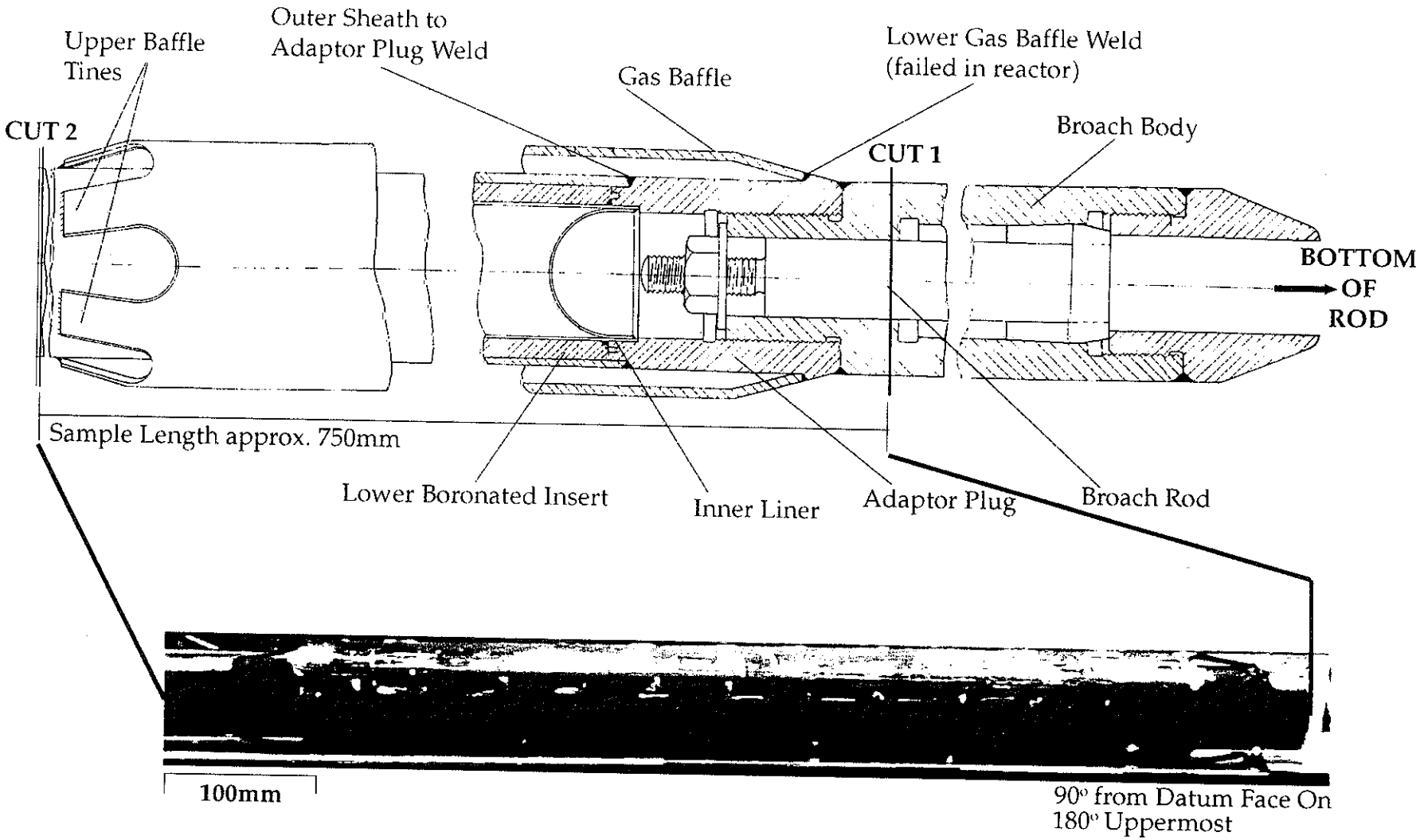

Figure 2: Sample of Bradwell Control Rod BR61 received into the caveline at Berkeley Centre with section of engineering drawing showing location of critical items for PIE.

Note: White markings were applied in-cave.

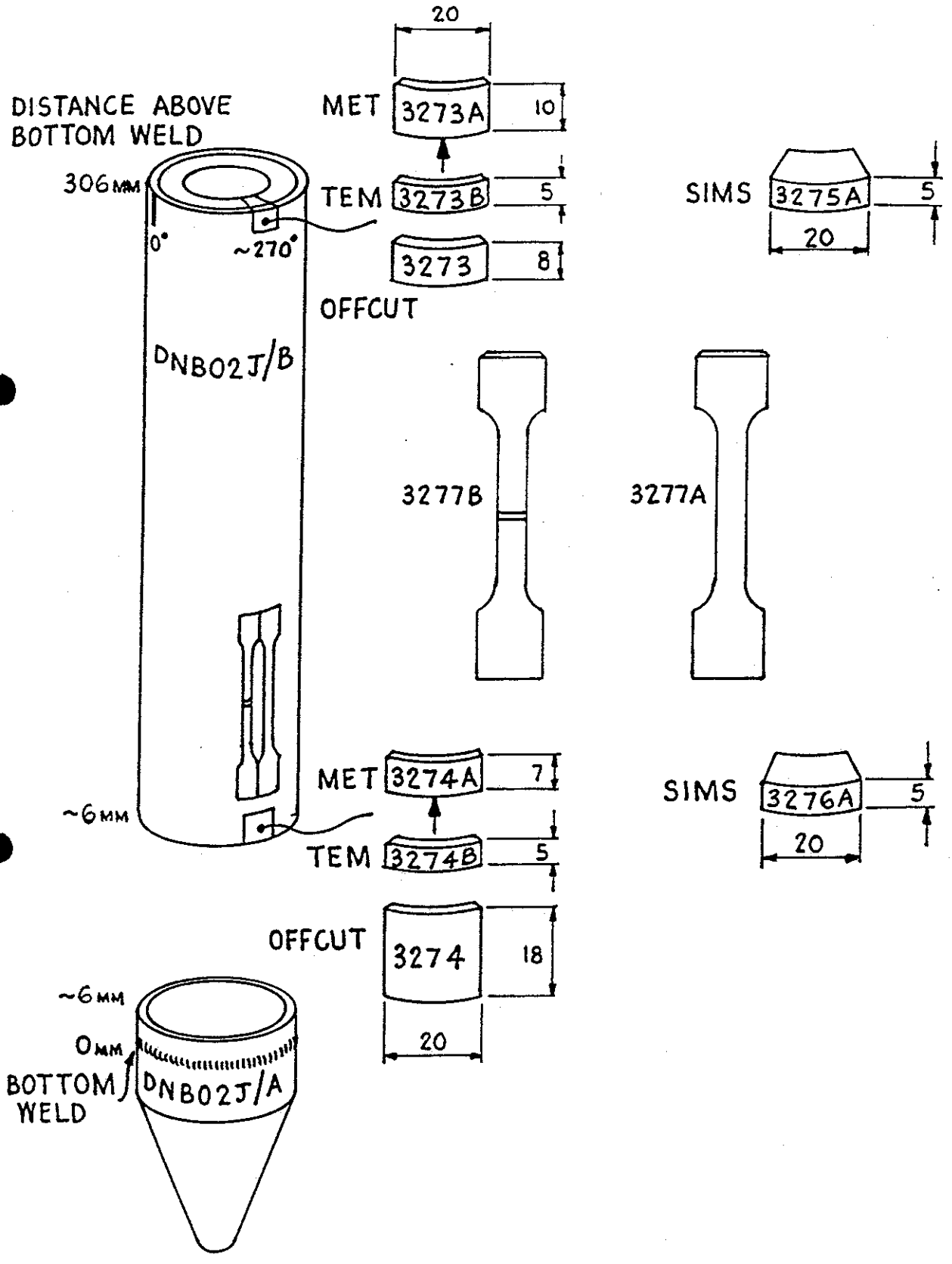

Figure 3: Cutting Diagram for Specimens from Dungeness A Control Rod 02J

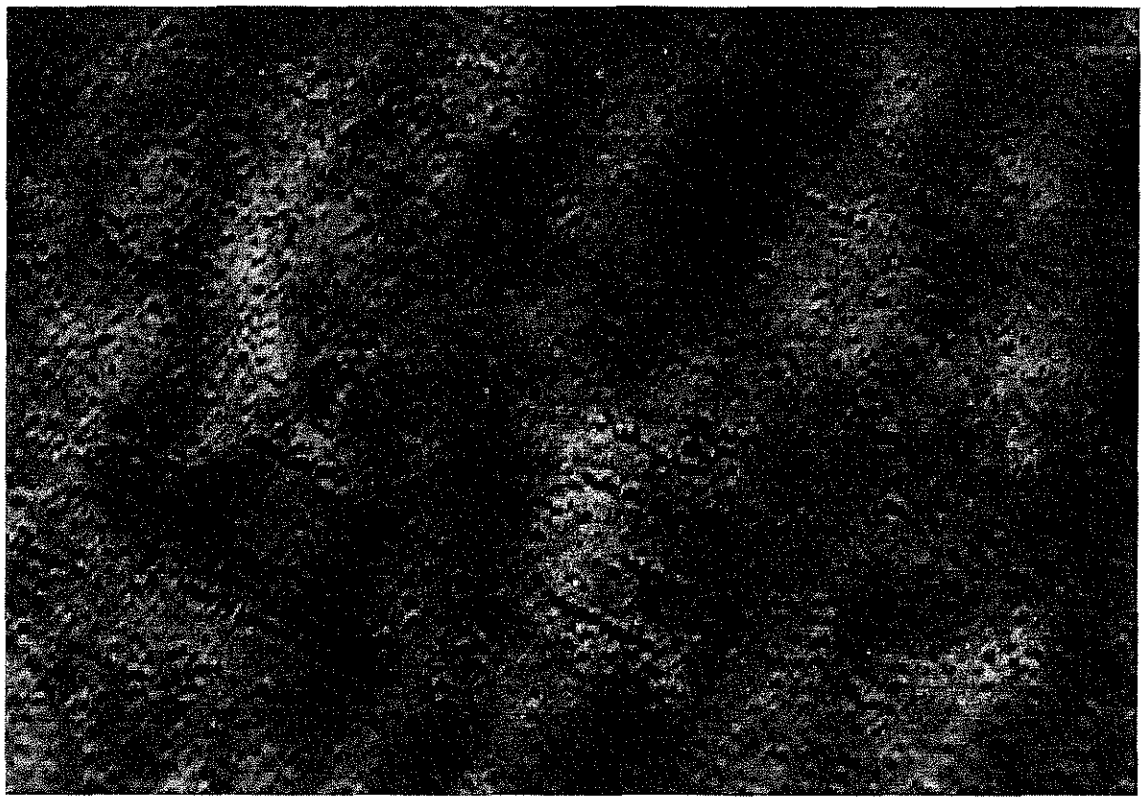

Figure 4: TEM Examination of Boron Insert Material Showing He Bubbles. Field Width 400nm

Transmission Electron Microscopy of Wylfa Control Rod

Images are 1/2,000 millimetre across

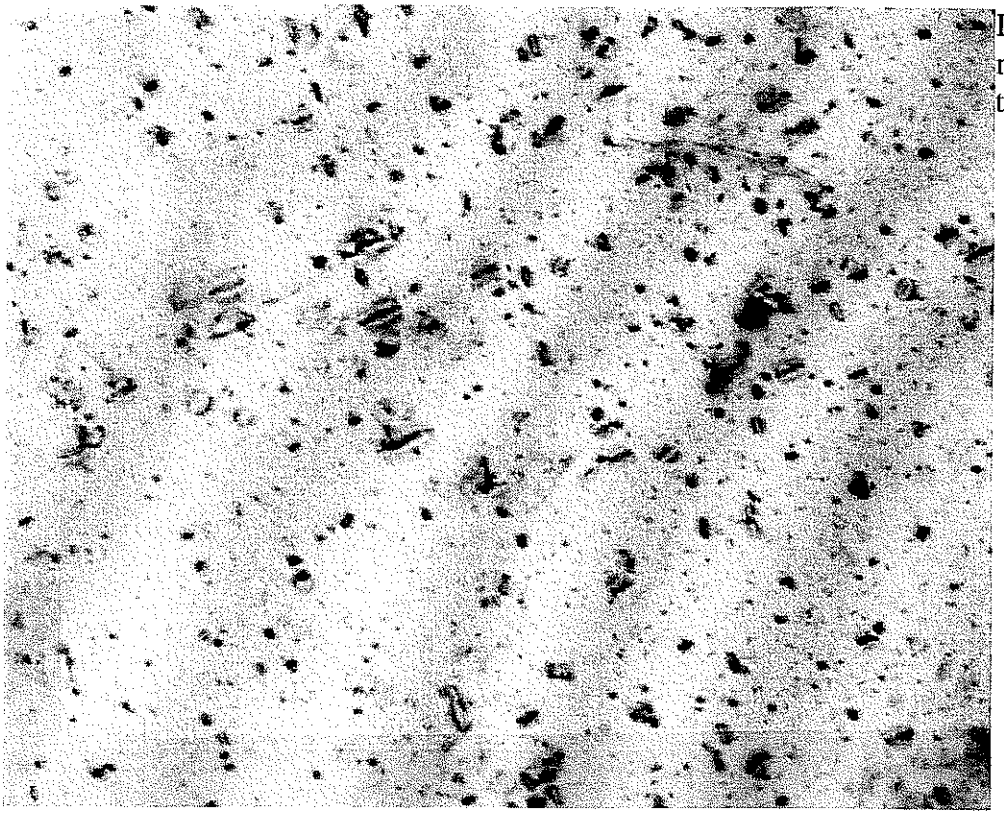

Damaged sheath material, operating temperature 285C.

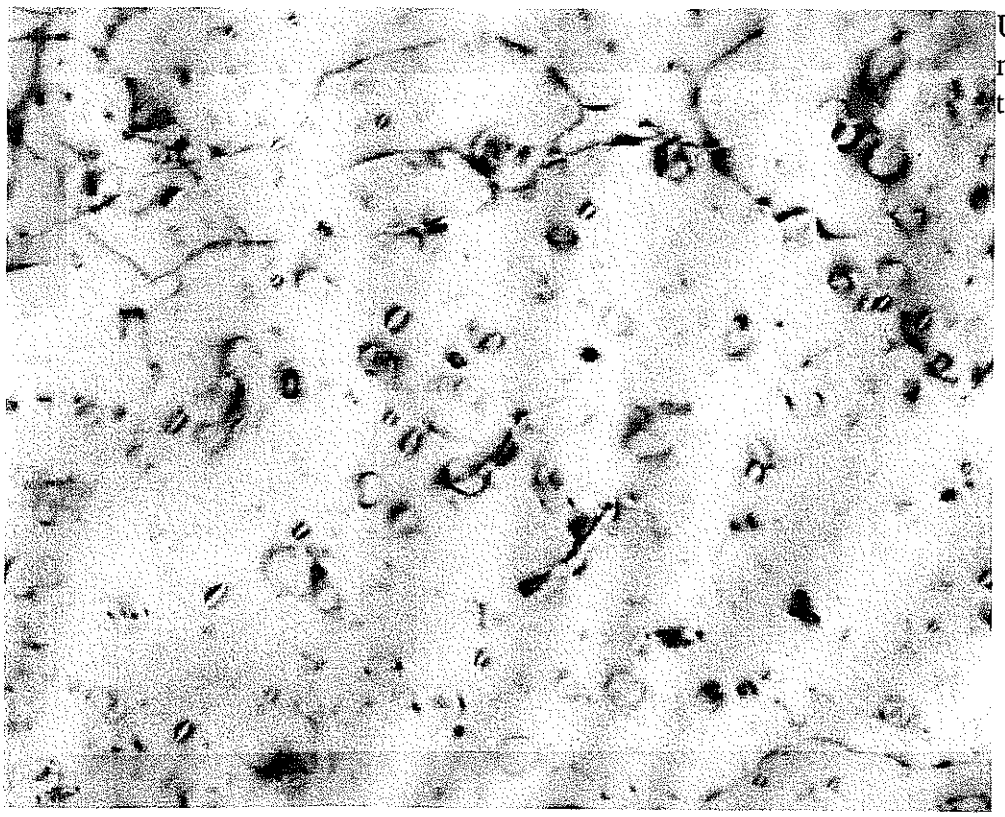

Undamaged sheath material, operating temperature 350C.

Figure 5: The damaged rod operating at an abnormally low temperature. Small copper particles and crystal defects have a strong embrittling effect and the sheath cannot absorb swelling of the boron steel insert without cracking. With fewer and larger microscopic features, the undamaged sheath material deforms without cracking. Measurement of copper particle size combined with a good theoretical understanding of their growth allows the operating temperature to be calculated.

Station 1

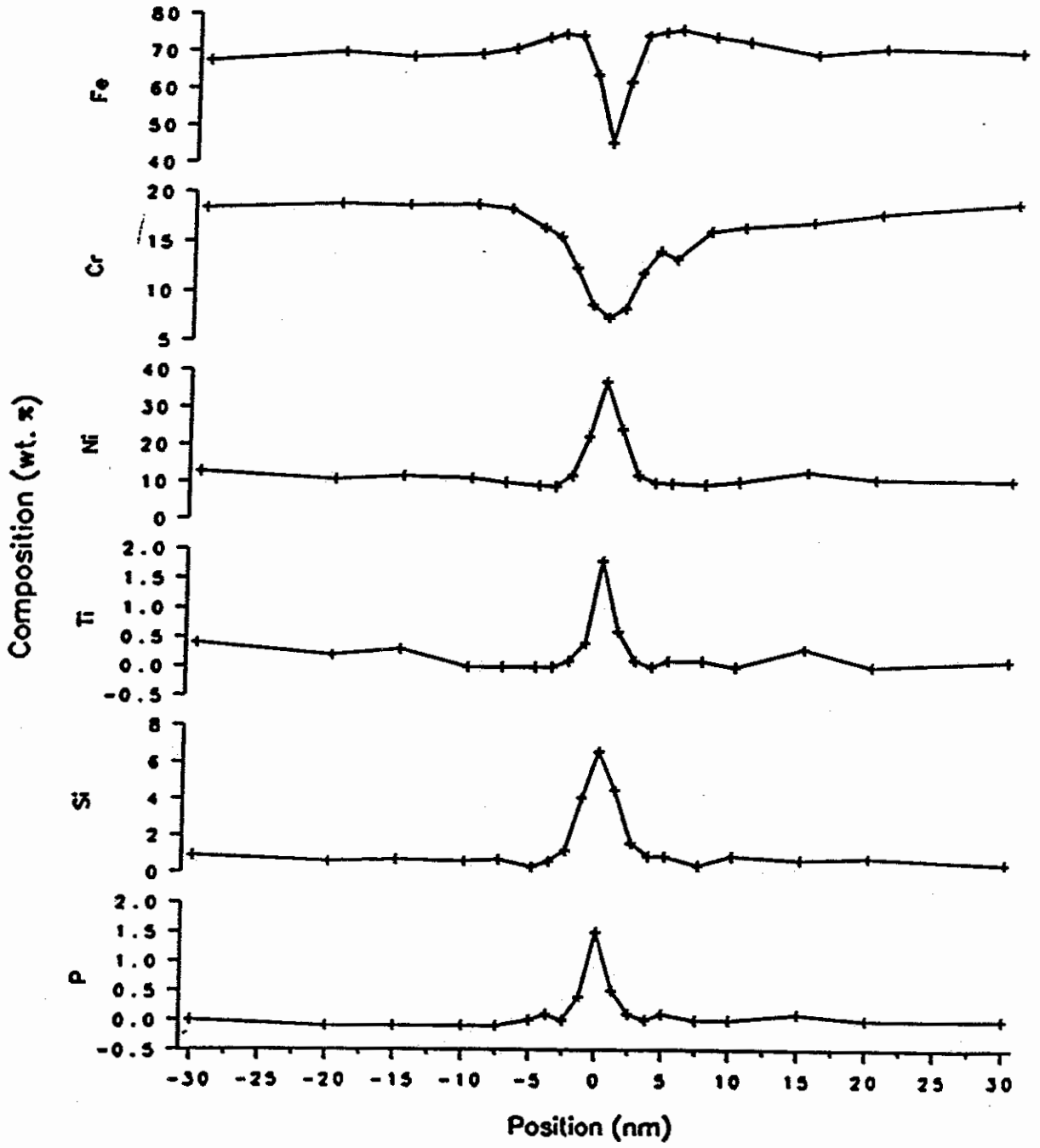

Figure 6: Grain boundary composition profiles from FEGSTEM analysis

Station 2

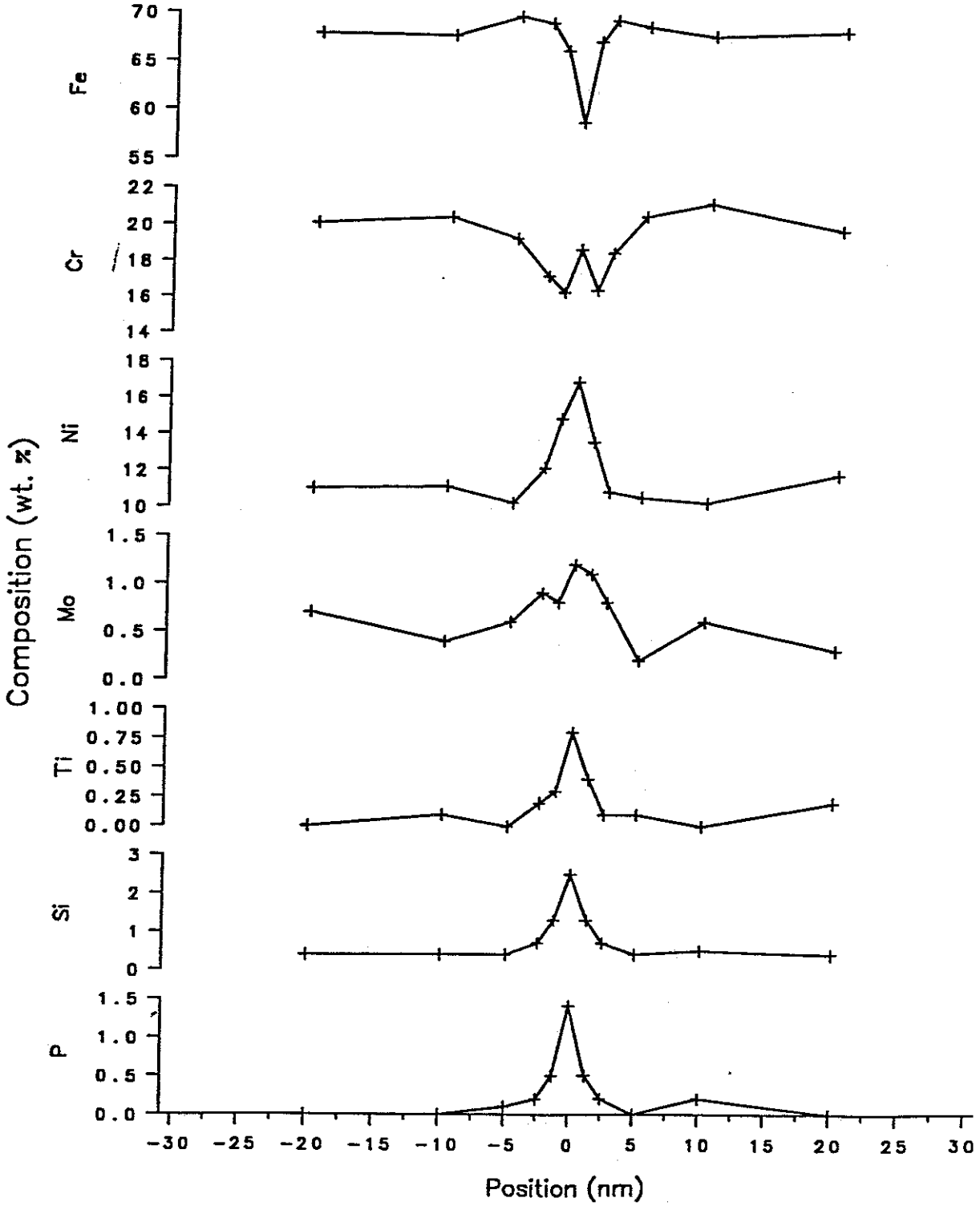

Figure 7: Grain boundary composition profiles from FEGSTEM analysis

Station 1

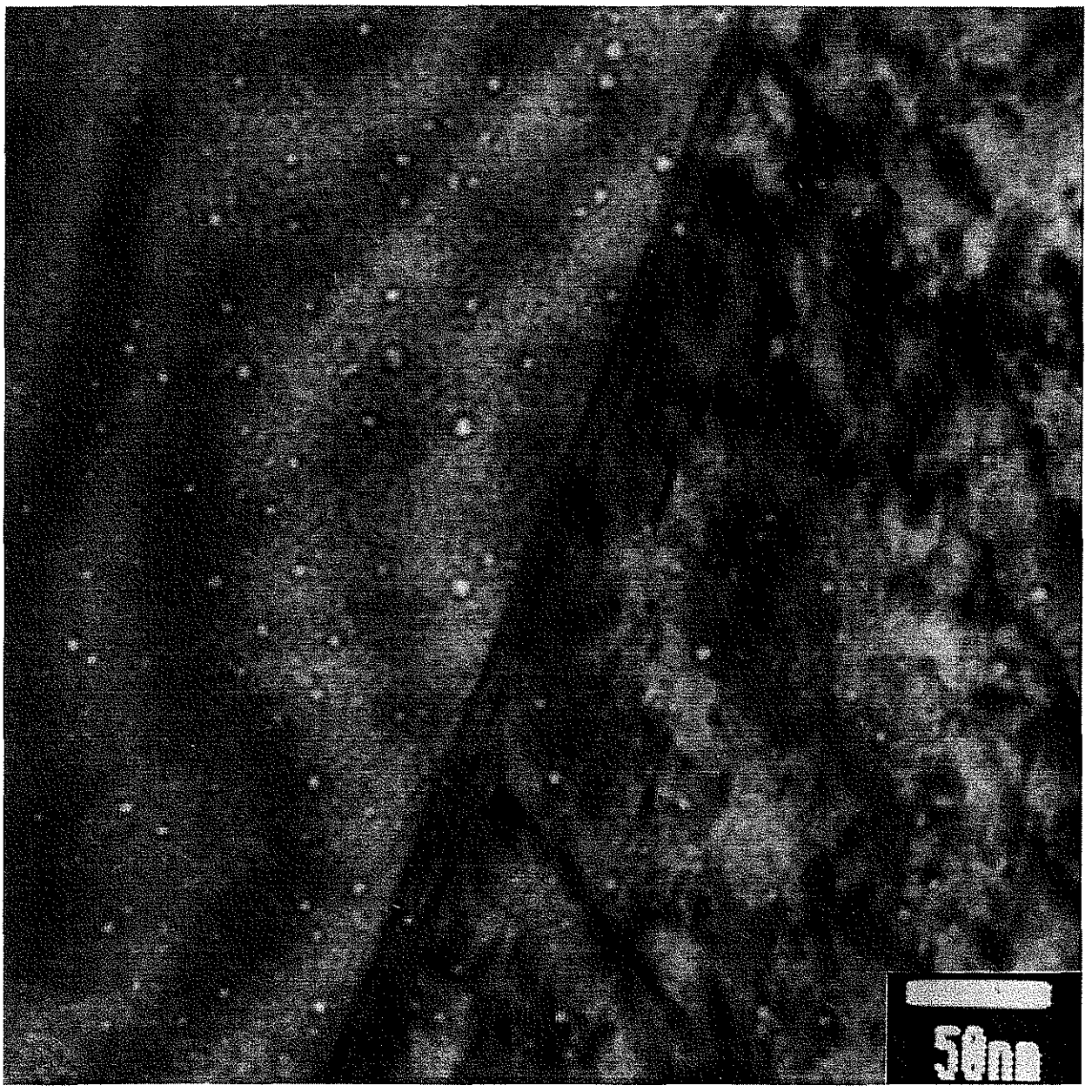

voids
size 2-6nm number density $9 \times 10^{21} m^{-3}$
volume fraction 0.03%

Figure 8: TEM Examination of Irradiated Stainless Steel Sheath Material